# Electronic structure and magnetic anisotropy of $CrO_2$

A. Toropova and G. Kotliar
*Center for Materials Theory, Department of Physics and Astronomy, Rutgers University, Piscataway, New Jersey 08854, USA*

S. Y. Savrasov
*Department of Physics, New Jersey Institute of Technology, Newark, New Jersey 07102, USA*

V. S. Oudovenko
*Bogoliubov Laboratory for Theoretical Physics, Joint Institute for Nuclear Research, 141980 Dubna, Russia*
*and Center for Materials Theory, Department of Physics and Astronomy, Rutgers University, Piscataway, New Jersey 08854, USA*
(Received 25 July 2004; revised manuscript received 18 January 2005; published 16 May 2005)

The problem of importance of strong correlations for the electronic structure, transport, and magnetic properties of half-metallic ferromagnetic $CrO_2$ is addressed by performing density functional electronic structure calculations in the local spin density approximation (LSDA) as well as using the LSDA+U method. It is shown that the corresponding low-temperature experimental data are best fitted without accounting for the Hubbard $U$ corrections. We conclude that the ordered phase of $CrO_2$ is weakly correlated.

DOI: 10.1103/PhysRevB.71.172403 PACS number(s): 75.30.Gw, 71.27.+a, 79.60.−i

As a compound with multiple industrial applications and its unusual half-metallic electronic structure, $CrO_2$ has recently attracted a lot of theoretical[1–6] and experimental[7–12] interest. The main discussion was centered around the role of strong correlations for the description of its ferromagnetic phase. Since Cr in its formal 4+ valence state has two 3$d$ electrons of $t_{2g}$ symmetry, one would expect manifestation of correlation effects of the Mott-Hubbard nature. On the other hand, metallic behavior of spin majority band suggests that Coulomb interactions of the Hubbard type can be screened out.[3] The comparison with the available photoemission and optical conductivity data did not make the situation more clear. One-electron spectra calculated using the LSDA+U method[13,14] fit well the photoemission and inverse photoemission experiments with the choice of intra-atomic Coulomb and exchange parameters $U=3$ eV and $J=0.87$ eV.[3,7] This indicates the importance of strong correlations. Contrary to this result, the LSDA optical conductivity calculations explain experimental data,[4] suggesting the regime of weak coupling.

In the present paper we address the issue of controversial role of strong correlations in ferromagnetic $CrO_2$ by presenting combined studies of its electronic structure, optical conductivity and magnetic anisotropy using the LSDA and LSDA+U schemes. We employ a linear-muffin-tin-orbital (LMTO) method in its atomic sphere approximation (ASA)[15,16] for our electronic structure calculations. The low symmetry of the rutile structure and small packing factor of the unit cell require an introduction of additional empty spheres. Their positions are chosen to be 4$c$ and 4$g$ in Wyckoff notations. The radii of the spheres (in atomic units) for Cr and O atoms, as well as of the empty spheres are chosen to be 1.975, 1.615, 1.378, and 1.434, correspondingly. The basis set adopted in the calculations is Cr$(4s,4p,3d)$ and O$(2s,2p)$.

In rutile structure Cr atoms are surrounded by distorted oxygen octahedra. The positions of the octahedra lead to a new natural basis for Cr orbitals. In this basis the cubic component of the octahedral crystal field splits the fivefold degenerate 3$d$ orbital into higher energy doubly degenerate $e_g$ level and lower energy triple degenerate $t_{2g}$ level. Distortions of oxygen octahedra further split the $t_{2g}$ states into lower energy $t_{2g}^{\parallel}$ orbital ($xy$ character) and higher energy twofold degenerate $t_{2g}^{\perp}$ orbitals ($yz+zx$ and $yz-zx$ characters).[3]

The results of the LSDA band structure calculation in the vicinity of the Fermi energy are shown in Figs. 1 and 2. The Fermi level crosses the spin majority $t_{2g}$ manifold. The rest of the Cr 3$d$ states is formed from four $e_g$ bands and three $t_{2g}$ spin minority bands which are located above the Fermi level. In both spin channels $e_g$ and $t_{2g}$ bands are well separated for all momenta except for the $\Gamma$ point. The whole 3$d$ complex is strongly hybridized with oxygen.

In Fig. 2 one can see that in the spin minority channel there is gap of approximately 1.3 eV between the oxygen 2$p$ band and the chromium 3$d$ band. This gap leads to 100% spin polarization at $E_F$ and assures the magnetic moment to be precisely equal to $4\mu_B$ per unit cell. The $t_{2g}$ bands that

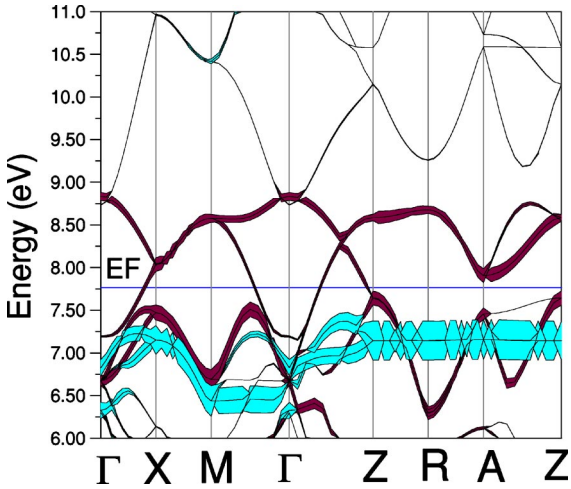


FIG. 1. (Color online) LSDA band structure of $CrO_2$ for spin majority carriers. Dark and light shaded areas (red and green) show the specific weight of $t_{2g}^{\perp}$ and $t_{2g}^{\parallel}$ orbitals, respectively, in the particular band.

 

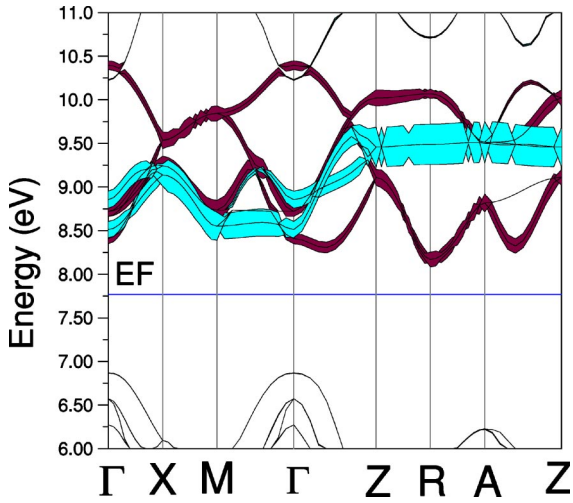


FIG. 2. (Color online) LSDA band structure of $CrO_2$ for spin minority carriers. Dark and light shaded areas (red and green) show the specific weight of $t_{2g}^{\perp}$ and $t_{2g}^{\parallel}$ orbitals, respectively, in the particular band.

cross the Fermi level in the spin majority channel mainly consist of the $t_{2g}^{\perp}$ orbitals (see Fig. 1). Almost nondispersive narrow band below $E_F$ (shown as lightly shaded) is formed by the $t_{2g}^{\parallel}$ orbital. This localized state undergoes large exchange splitting $\Delta^{ex}$ making spin minority $t_{2g}^{\parallel}$ orbitals unoccupied (see Fig. 2).

The main changes which occur in the band structure for nonzero values of $U$ and $J$ using the LSDA+U method are schematically shown in Fig. 3. These calculations were performed with $U=3$ eV and $J=0.87$ eV. The center of gravity of occupied $t_{2g}^{\parallel}$ band is pushed down by 0.6 eV. The spin majority unoccupied $e_g$ bands are pushed up by 0.6 eV, which opens 0.4 eV gap between $t_{2g}^{\perp}$ and $e_g$ bands above the Fermi level. In the spin minority channel the occupied oxygen bands are shifted up by 0.3 eV. The upper unoccupied $t_{2g}$ and $e_g$ bands are shifted up by 1.1 eV. As a result, the insulating gap is increased and reaches the value of 2.1 eV.

Before we proceed we would like to compare our results with earlier reported calculations. Table I summarizes values of spin minority energy gap $\Delta$ and exchange splitting $\Delta_{ex}$, reported in literature as well as the ones obtained by us. We would like to emphasize that our results obtained using ASA

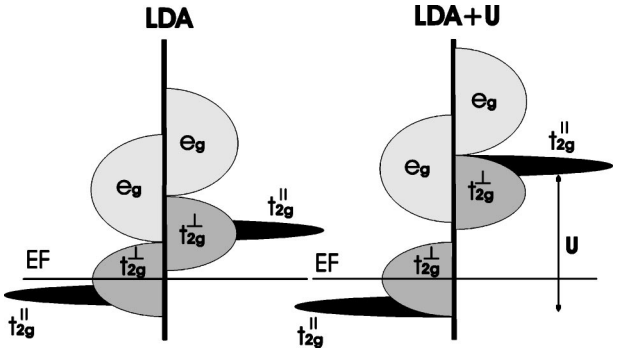


FIG. 3. Schematic density of states (DOS) of $CrO_2$ deduced from the LSDA and LSDA+U calculations. Shaded semicircles from right and left represent the bands for spin majority and spin minority carriers.

TABLE I. Values of the energy gap $\Delta$ and the exchange splitting $\Delta_{ex}$ (in eV) in b–e are approximate and extracted from DOS reported in the papers cited below.

| | LSDA[a] | LSDA+U[a] | LSDA[b] | LSDA+U[c] | GGA[d] | GGA[e] |
|---|---|---|---|---|---|---|
| $\Delta$ | 1.3 | 2.1 | 1.5 | 2.0 | 1.3 | 1.8 |
| $\Delta_{ex}$ | 2.3 | 4.6 | 1.8 | 4.5 | 2.5 | 2.9 |

[a]Our calculations.
[b]As reported by Schwartz (Ref. 1).
[c]As reported by Korotin *et al.* (Ref. 3).
[d]As reported by Mazin *et al.* (Ref. 4).
[e]As reported by Kunes *et al.* (Ref. 10).

are in the excellent agreement with full potential calculations performed by Mazin and co-workers.[4]

Now we compare calculated electronic structure using the LSDA and the LSDA+U methods with the available experimental data. Figure 4 shows comparison of ultraviolet photoemission spectroscopy (UPS) experiments[7] (photon energy $h\nu=40.8$ eV) with the theoretical spectra which are calculated densities of states smeared by both Gaussian and Lorentzian broadening functions. The Gaussian broadening takes into account experimental resolution while Lorentzian takes into account finite lifetime effects. The Gaussian broadening parameter is taken to be 0.4 eV. The full width at half-maximum (FWHM) of the Lorentzian was taken to be energy dependent and equal to $0.2|E-E_F|$ eV. We can distinguish two main features in the UPS spectra: (i) a small hump in around $-1.5$ eV which arises from the $t_{2g}$ band of Cr, and (ii) a big hump around $-6.0$ eV which comes from the broad $2p$ oxygen band. Both features are fairly well described by both the LSDA and the LSDA+U calculation. The small discrepancy between the LSDA calculation and experiment could be referred to the fact that at small photon energies photoemission is a more surface sensitive technique. Indeed, recent PES studies of Vanadium oxides[17] have been found to yield spectra not characteristic of the bulk, but rather of surface atoms whose lower coordination number can render more strongly correlated surface layer.

For the unoccupied states we have chosen to compare our

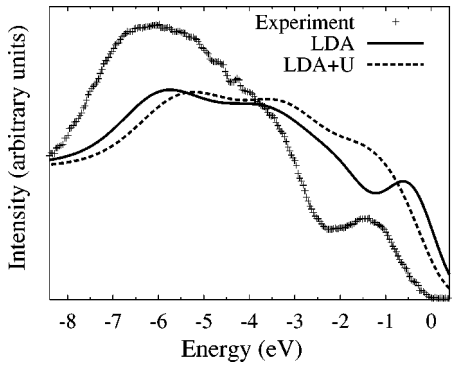


FIG. 4. Comparison between theoretical densities of states and experimental (Ref. 7) UPS spectra for $CrO_2$. The theoretical DOS were smeared out by Gaussian and Lorentzian broadening functions to account for experimental resolution and lifetime effects. The secondary electron background has been taken into account.

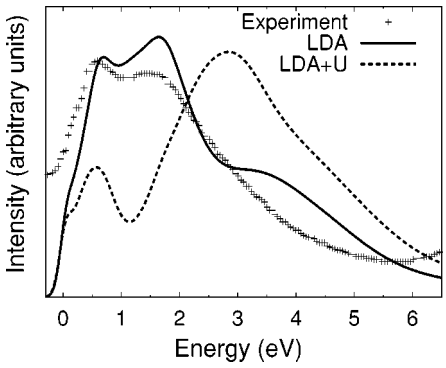


FIG. 5. Comparison between theory and experiment (Ref. 11) for Cr $2p$ x-ray absorption (XAS) spectrum. To deduce theoretical curve from the partial Cr $3d$ and $4s$ DOS we used 0.1 eV for Gaussian FWHM. The Lorentzian FWHM was taken to be energy dependent and equal to $0.2|E-E_F|$. The binding energy of core $2p_{3/2}$ Cr state 577 eV has been subtracted from the experimental spectrum.

results with the available x-ray absorption spectra (XAS)[11] rather than with the inverse photoemission as it had been done before.[7] The main reason for this is that XAS is a bulk (not surface) sensitive method. The $2p$ Cr XAS spectrum[11] is compared to our theoretical calculations in Fig. 5. To deduce theoretical spectra we performed both Gaussian and Lorentzian broadening of $3d$ and $4s$ partial DOS. Two first peaks around 0.5 eV and around 1.5 eV come from the unoccupied $3d$ orbitals of chromium. The main contribution to the second peak comes from the $t_{2g}$ orbitals in the spin minority channel. Thus, the LSDA+U overestimates the spin minority gap twice as much.

Below we discuss the optical conductivity of $CrO_2$. In Fig. 6 diagonal $x$ components of the optical conductivity calculated using the LSDA and LSDA+U methods are compared with the experimental results reported by Basov and co-workers[8] ($x$ coordinate refers to the basis of unit cell). The main two features of the calculated optical conductivity are a shoulder around 2–3 eV and a broad hump located at energies 0.2–1.5 eV. In both LSDA and LSDA+U schemes the shoulder can be identified with two types of transitions. First contribution arises from the minority spin gap transitions and the second one comes from transitions between the occupied

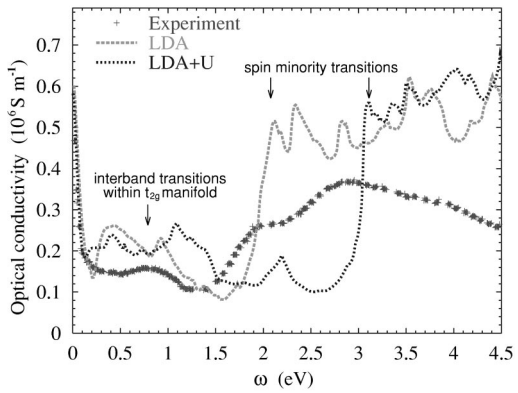


FIG. 6. (Color online) Comparison of the optical conductivity of $CrO_2$ obtained using the LSDA and LSDA+U methods against the experimental data (Ref. 8).

$t_{2g}^{\parallel}$ and unoccupied $e_g$ bands. The hump is formed by interband transitions within the $t_{2g}$ manifold and the oxygen $2p$ bands near the Fermi level in the spin majority channel. Apparently, the LSDA prediction is much closer to the experimental curve than the LSDA+U one. The LSDA+U calculations overestimate the minority gap, and hence, the spin minority transitions occur at higher energies. Our conclusion completely agrees with the conclusion of the study by Mazin and co-workers.[4]

Results of calculated MAE for $CrO_2$ are presented below. We remind that magnetic anisotropy is the dependence of the internal energy on the direction of spontaneous magnetization. The magnetic anisotropy is a relativistic phenomenon arising due to spin-orbit coupling, where the spin degrees of freedom interact with the spatial anisotropy through the coupling to the orbital degrees of freedom. The experimental measurement of MAE for $CrO_2$ were labored by the fact that chromium dioxide is a metastable compound, which irreversibly decomposes at about 200 °C.[18] The recent reliable measurements are performed on epitaxial $CrO_2$ layers.[19–21] For thicker films (700 Å–1.2 $\mu$m) the in-plane magnetic anisotropy was observed with [001] and [010] easy and hard axis directions, respectively. The value of magnetocrystalline anisotropy constant $K_1$ reported by different groups are 6.7 $\mu$eV,[19] 9.6 $\mu$eV,[20] and 15.6 $\mu$eV (Ref. 21) per cell. These values are bigger than typical values of MAE for metals (e.g., for Ni and Fe they are 2.8 and 1.4 $\mu$eV per cell correspondingly[25]). It could be justified by the fact that such metals as Fe and Ni have cubic crystal structure where MAE identically vanishes in the second order and arises as fourth order effect in the spin-orbit coupling.[25] The low crystal symmetry of $CrO_2$ provides MAE to appear already in the second order of the perturbation theory, leading to bigger value of MAE than typical metal values.

Within our LSDA calculation the direction [001] was found to be easy magnetization axis, which is consistent with latest thin film experiments.[19–21] To calculate the magnetic anisotropy energies (MAEs) we subtract the total energy for easy magnetization axis from the total energies with different directions of magnetization ([010], [111], and [102]). For the momentum space integration in the total energy calculations, we follow the analysis given by Trygg and co-workers[22] and use special point method[23] with a Gaussian broadening[24] of 15 m Ry. The validity and convergence of this procedure has been tested in their work.[22] We used about 1000 **k** points in the irreducible Brillouin zone, while the convergence of MAE was tested up to 8000 **k** points without any change in values of MAE. Numerical values of MAE in LSDA calculation exceed the maximum experimental value by approximately four times.[21]

To figure out the influence of intra-atomic repulsion $U$ on the magnetic anisotropy, we have performed LSDA+U calculations for different values of $U$ increasing it from 0 to 6 eV ($J=0.87$ eV was kept constant except for the LSDA $U=0$ case). The results of these calculations are presented in Fig. 7. MAE decreases rapidly starting from the LSDA value (which is approximately equal to 68 $\mu$eV per cell) and changes its sign around $U\approx 0.9$ eV. This leads to switching correct easy magnetization axis [001] to the wrong one, namely [102]. The biggest experimental value of the MAE

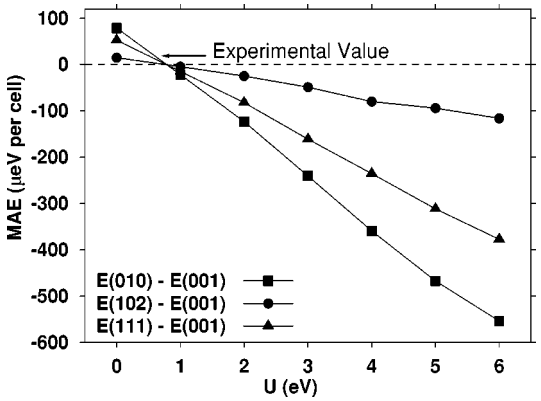


FIG. 7. The magnetocrystalline anisotropy energies for $CrO_2$ as functions of $U$. The experimental value of MAE $E[010]-E[001]=15.6$ $\mu$eV per cell is shown by the arrow.

reported in the literature is 15.6 $\mu$eV per cell.[21] The calculated MAE approaches this value around $U=0.6$ eV. This signals that correlation effects in the $d$ shell may be important for this compound although they are strongly screened out.

Another question can arise whether dynamical mean field theory (DMFT) treatment would change values of MAE or not. From our experience we expect the total energy to be sufficiently robust quantity, almost insensitive to the fact whether we take into account dynamical correlations or not. Within DMFT framework the redistribution of the spectral weight nearby the Fermi level usually occurs, but the total energy seems to remain almost the same.

To conclude, we have reported the LSDA and LSDA+U calculations of electronic structure, optical conductivity, and magnetic anisotropy of $CrO_2$. Our comparisons with the experimental data point out the local spin density approximation as the proper method to describe this material. We explained the discrepancy between the LSDA and photoemission studies, discussed earlier by other authors,[3,7] by the fact that due to small photon energies used in PES, it is more surface rather than bulk sensitive technique. We resolved this problem by showing that XAS spectrum is unambiguously described by the LSDA calculation. It has been also shown that even intermediate values of $U$ (of the order of 1–2 eV) lead to the failure of the LSDA+U method to describe the magnetic anisotropy and the optical conductivity of $CrO_2$. Since the LSDA+U is not adequate for the description of electronic structure of $CrO_2$ as well as of its optical and magnetic properties, we conclude that the ordered phase of $CrO_2$ could be described as weakly correlated material with small values of on-site Coulomb repulsion. It is important to notice that, while we have found that a simple one-electron picture describes well the ferromagnetic phase of this material, there is a narrow band formed by the nondispersive $t_{2g}^{\|}$ orbitals ($xy$ character) which in the paramagnetic phase will be single occupied, due to the on-site Coulomb interactions, an effect which cannot be described in LDA and will require a dynamical mean-field treatment for this material as done in Ref. 5. The physical basis for the applicability of static mean-field picture in the *ferromagnetic phase* of this material, is due to the large exchange splitting which is able to effectively enforce the single occupancy of the $t_{2g}^{\|}$ orbitals.

This research was supported by the ONR Grant No. 4-2650. The authors would like to thank I. I. Mazin.

[1] K. Schwarz, J. Phys. F: Met. Phys. **16**, L211 (1986).
[2] S. P. Lewis, P. B. Allen, and T. Sasaki, Phys. Rev. B **55**, 10253 (1997).
[3] M. A. Korotin, V. I. Anisimov, D. I. Khomskii, and G. A. Sawatzky, Phys. Rev. Lett. **80**, 4305 (1998).
[4] I. I. Mazin, D. J. Singh, and C. Ambrosch-Draxl, Phys. Rev. B **59**, 411 (1999).
[5] M. S. Laad, L. Craco, and E. Müller-Hartmann Phys. Rev. B **64**, 214421 (2001).
[6] L. Craco, M. S. Laad, and E. Müller-Hartmann Phys. Rev. Lett. **90**, 237203 (2003).
[7] T. Tsujioka, T. Mizokawa, J. Okamoto, A. Fujimori, M. Nohara, H. Takagi, K. Yamaura, and M. Takano, Phys. Rev. B **56**, R15509 (1997).
[8] E. J. Singley, C. P. Weber, D. N. Basov, A. Barry, and J. M. D. Coey, Phys. Rev. B **60**, 4126 (1999).
[9] C. B. Stagarescu, X. Su, D. E. Eastman, K. N. Altmann, F. J. Himpsel, and A. Gupta, Phys. Rev. B **61**, R9233 (2000).
[10] J. Kuneš, P. Novák, P. M. Oppeneer, C. König, M. Fraune, U. Rüdiger, G. Güntherodt, and C. Ambrosch-Draxl, Phys. Rev. B **65**, 165105 (2002).
[11] E. Z. Kurmaev, A. Moewes, S. M. Butorin, M. I. Katsnelson, L. D. Finkelstein, J. Nordgren, and P. M. Tedrow, Phys. Rev. B **67**, 155105 (2003).
[12] D. J. Huang, H.-T. Jeng, C. F. Chang, G. Y. Guo, J. Chen, W. P. Wu, S. C. Chung, S. G. Shyu, C. C. Wu, H.-J. Lin, and C. T. Chen, Phys. Rev. B **66**, 174440 (2002).
[13] V. I. Anisimov, F. Aryastiawan, and A. I. Lichtenstein, J. Phys.: Condens. Matter **9**, 767 (1997).
[14] For a review, see, e.g., *Strong Correlations in Electronic Structure Calculations*, edited by V. I. Anisimov (Gordon and Breach Science Publishers, Amsterdam, 2000).
[15] O. K. Andersen Phys. Rev. B **12**, 3060 (1975).
[16] S. Y. Savrasov, Phys. Rev. B **54**, 16470 (1996).
[17] S.-K. Mo, J. D. Denlinger, H.-D. Kim, J.-H. Park, J. W. Allen, A. Sekiyama, A. Yamasaki, K. Kadono, S. Suga, Y. Saitoh, T. Muro, P. Metcalf, G. Keller, K. Held, V. Eyert, V. I. Anisimov, and D. Vollhardt, Phys. Rev. Lett. **90**, 186403 (2003).
[18] B. L. Chamberland, CRC Crit. Rev. Solid State Mater. Sci. **7**, 1 (1977).
[19] L. Spinu, H. Srikanth, A. Gupta, X. W. Li, and Gang Xiao, Phys. Rev. B **62**, 8931 (2000).
[20] F. Y. Yang, C. L. Chien, E. F. Ferrari, X. W. Li, Gang Xiao, and A. Gupta, Appl. Phys. Lett. **77**, 286 (2000).
[21] X. W. Li, A. Gupta, and Giang Xiao, Appl. Phys. Lett. **75**, 713 (1999).
[22] J. Trygg, B. Johansson, O. Eriksson, and J. M. Wills, Phys. Rev. Lett. **75**, 2871 (1995).
[23] S. Froyen, Phys. Rev. B **39**, 3168 (1989).
[24] M. Methfessel and A. T. Paxton, Phys. Rev. B **40**, 3616 (1989).
[25] I. Yang, S. Y. Savrasov, and G. Kotliar, Phys. Rev. Lett. **87**, 216405 (2001).